Chapter 8

New Horizons

The focus of the previous chapters has been on approximate models for use in general engineering applications. Throughout this text, we have stressed the virtue of using the minimum amount of complexity while capturing the essence of the relevant physics. This is the same notion that G. I. Taylor described as the "simple model/simple experiment" approach. Nevertheless, no pretense has been made that any of the models devised in this spirit applies universally to all turbulent flows. We must always proceed with some degree of caution since there is no guarantee that such models are accurate beyond their established data base. Thus, while simplicity has its virtues for many practical engineering applications, there is a danger that must not be overlooked. Specifically, as quipped by H. L. Mencken, "to every difficult question there is a simple answer — which is wrong."

This chapter discusses modern efforts that more directly address the physics of turbulence without introducing Reynolds closure approximations. We begin by discussing Direct Numerical Simulation (DNS) in which the exact Navier-Stokes and continuity equations are solved, albeit at relatively low Reynolds numbers. Next, we turn to Large Eddy Simulation (LES) in which the largest eddies are computed exactly and the smallest eddies are modeled, hopefully with a non-critical impact on the simulation. Finally, we discuss current efforts in chaos studies, and their possible relevance to turbulence.

8.1 Background Information

Before plunging into these topics, it is worthwhile to pause and discuss certain aspects of turbulence that we haven't explicitly addressed in preceding

chapters. The first important point we must consider is that of the smallest scales of turbulence. Our primary focus in devising closure approximations has been on the dynamics of the largest eddies, which account for most of the transport of properties in a turbulent flow. Our use of dimensional analysis, in which molecular viscosity has been ignored, guarantees that the closure approximations involve length scales typical of the energy-bearing eddies whose Reynolds number — however defined — is much larger than one except close to a solid surface, i.e., in the viscous wall region, $y^+ < 3$, say. (This is the reason that viscous damping functions are often needed close to a solid boundary where the dissipating eddies dominate, and even the energy-bearing eddies have Reynolds numbers of order one.) To achieve a more complete description of turbulence, we must determine what the smallest length scale in a turbulent flow is.

Interestingly, we can estimate the magnitude of the smallest scales by again appealing to dimensional analysis. Of course, to establish the relevant dimensional parameters, we must first consider the physics of turbulence at very small length scales. We begin by recalling that the cascading process present in all turbulent flows involves a transfer of kinetic energy from larger eddies to smaller eddies. Dissipation of kinetic energy to heat through the action of molecular viscosity occurs at the scale of the smallest eddies. Because small-scale motion tends to occur on a short time scale, we can reasonably assume that such motion is independent of the relatively slow dynamics of the large eddies and of the mean flow. Hence, the smaller eddies should be in a state where the rate of receiving energy from the larger eddies is very nearly equal to the rate at which the smallest eddies dissipate the energy to heat. This is known as Kolmogorov's (1941) **universal equilibrium theory**, a corollary of which is his **hypothesis of local isotropy** that we appealed to in developing some of the closure approximations in Chapter 6. Hence, the motion at the smallest scales should depend only upon: (a) the rate at which the larger eddies supply energy, ϵ, and (b) the kinematic viscosity, ν.

Having established ϵ and ν as the appropriate dimensional parameters, it is a simple matter to form the following length (η), time (τ) and velocity (v) scales.

$$\eta \equiv (\nu^3/\epsilon)^{1/4}, \quad \tau \equiv (\nu/\epsilon)^{1/2}, \quad v \equiv (\nu\epsilon)^{1/4} \tag{8.1}$$

These are the **Kolmogorov scales** of length, time and velocity. To appreciate how small the Kolmogorov length scale is for example, recall that the length scale appropriate to the energy-bearing eddies, ℓ, (often referred to as the **integral scale** in statistical turbulence theory) is related to ϵ by

Equation (4.8), so that

$$\frac{\eta}{\ell} \sim Re_T^{-3/4} \tag{8.2}$$

where $Re_T = k^{1/2}\ell/\nu$ is the usual turbulence Reynolds number. Since values of Re_T in excess of 10^4 are typical of fully-developed turbulent boundary layers and $\ell \sim 0.1\delta$ where δ is boundary-layer thickness, the Kolmogorov length scale, η, outside the viscous wall region is less than one ten-thousandth times the thickness of the boundary layer.

Another turbulence length scale often referred to in the statistical theory of turbulence is the **Taylor microscale**, λ [c.f., Tennekes and Lumley (1983) or Hinze (1975)]. For isotropic turbulence, it is defined by

$$\epsilon = 15\nu\overline{\left(\frac{\partial u'}{\partial x}\right)^2} \equiv 15\nu\frac{\overline{u'^2}}{\lambda^2} \tag{8.3}$$

Again, using Equation (4.8), and assuming $k \sim \overline{u'^2}$, we conclude that

$$\frac{\lambda}{\ell} \sim Re_T^{-1/2} \quad \text{or} \quad \lambda \sim (\ell\eta^2)^{1/3} \tag{8.4}$$

Thus, in general we can say that for high-Reynolds-number turbulence there is a distinct separation of these scales, i.e.,

$$\eta \ll \lambda \ll \ell \tag{8.5}$$

Results of numerical simulations are often characterized in terms of the **microscale Reynolds number**, Re_λ, defined by

$$Re_\lambda = k^{1/2}\lambda/\nu \tag{8.6}$$

Finally, the **eddy turnover time**, $\tau_{turnover}$, is simply the ratio of the macroscales for length, ℓ, and velocity, $k^{1/2}$, and is given by

$$\tau_{turnover} \sim \ell/k^{1/2} \tag{8.7}$$

The eddy turnover time is a measure of the time it takes an eddy to interact with its surroundings. It is also the reciprocal of the specific dissipation rate, ω.

A second important consideration is the spectral representation of turbulence properties. That is, since turbulence contains a continuous spectrum of scales, it is often convenient to cast our analysis in terms of the **spectral distribution** of energy. If κ denotes wavenumber and $E(\kappa)d\kappa$ is the turbulence kinetic energy contained between wavenumbers κ and $\kappa+d\kappa$, we can say

$$k \equiv \frac{1}{2}\overline{u_i'u_i'} = \int_0^\infty E(\kappa)\,d\kappa \tag{8.8}$$

Recall that k is half the trace of the autocorrelation tensor, $\mathcal{R}_{ij}$, defined in Equation (4.50). Correspondingly, the **energy spectral density** or **energy spectrum function**, $E(\kappa)$, is the Fourier transform of half the trace of $\mathcal{R}_{ij}$. In general, we regard a spectral representation as a decomposition into wavenumbers (κ) or, equivalently, wavelengths ($2\pi/\kappa$). See Tennekes and Lumley (1983) for a detailed discussion of energy spectra. In the present context, we think of the reciprocal of κ as the eddy size.

In general, $E(\kappa)$ is a function of ν, ϵ, ℓ, κ and the mean strain rate, S. We needn't consider k as it can be expressed in terms of ϵ and ℓ. As part of his universal equilibrium theory, Kolmogorov also made the hypothesis that for very large Reynolds number, there is a range of eddy sizes between the largest and smallest for which the cascade process is independent of the statistics of the energy-containing eddies (so that S and ℓ can be ignored) and of the direct effects of molecular viscosity (so that ν can be ignored). The idea is that a range of wavenumbers exists in which the energy transferred by inertial effects dominates, wherefore $E(\kappa)$ depends only upon ϵ and κ. On dimensional grounds, he thus concluded that

$$E(\kappa) = C_K \epsilon^{2/3} \kappa^{-5/3}, \qquad \frac{1}{\ell} \ll \kappa \ll \frac{1}{\eta} \tag{8.9}$$

where C_K is the Kolmogorov constant. Because inertial transfer of energy dominates, Kolmogorov identified this range of wavenumbers as the **inertial subrange**. The existence of the inertial subrange has been verified by many experiments and numerical simulations, although many years passed before definitive data were available to confirm its existence. Figure 8.1 shows a typical energy spectrum for a turbulent flow.

The Kolmogorov -5/3 law is so well established that, as noted by Rogallo and Moin (1984), theoretical or numerical predictions are regarded with skepticism if they fail to reproduce it. Its standing is as important as the law of the wall. With these preliminary remarks in hand, we are now in a position to discuss DNS and LES in the next two sections.

8.2 Direct Numerical Simulation

A direct numerical simulation, or DNS for short, means a complete time-dependent solution of the Navier-Stokes and continuity equations. The value of such simulations is obvious. From a practical standpoint, computed statistics can be used to test proposed closure approximations in engineering models. At the most fundamental level, they can be used to obtain understanding of turbulence structure and processes that can be of value in developing turbulence control methods (e.g., drag reduction) or prediction

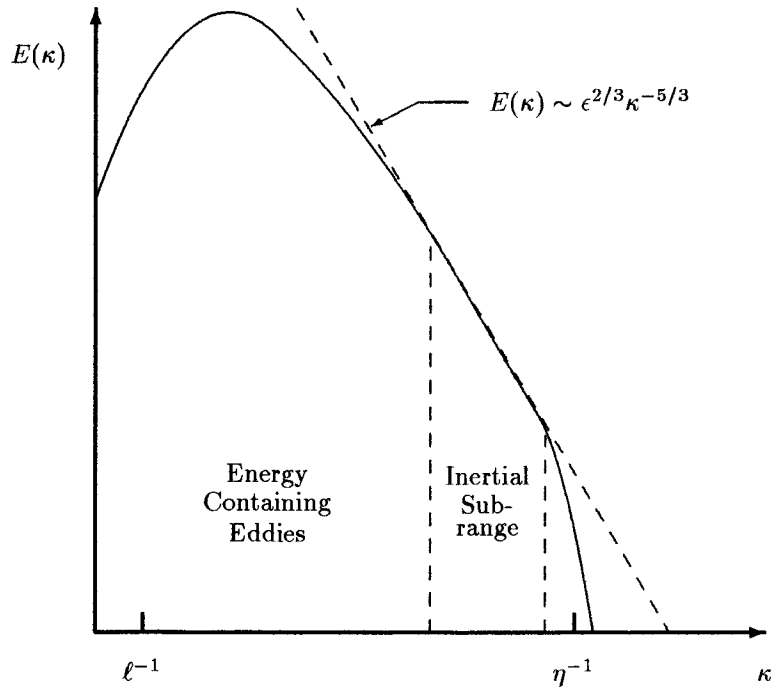

Figure 8.1: Energy spectrum for a turbulent flow — log-log scales.

methods. They can also be viewed as an additional source of experimental data that have been taken with unobtrusive measuring techniques. This is especially desirable in obtaining information about essentially unmeasurable properties like pressure fluctuations.

All of these comments assume the DNS is free of significant numerical, and other, forms of error. This is a nontrivial consideration, and the primary concerns in DNS are related to numerical accuracy, specification of boundary and initial conditions, and making optimum use of available computer resources. This section will discuss these issues briefly. For more detail at an introductory level, see the excellent (although a bit dated) review article by Rogallo and Moin (1984).

Estimating the number of grid points and timesteps needed to perform an accurate DNS reveals the complexity of the problem from a computational point of view. As an example, consider incompressible turbulent flow in a channel of height H. The computational domain must be of sufficient extent to accommodate the largest turbulence scales. In channel flow, eddies are elongated in the direction parallel to the channel walls, and their

length Λ is known to be about $2H$. Also, in principle, the grid must be fine enough to resolve the smallest eddies whose size is of the order of the Kolmogorov length scale, η. Assuming that at least 4 grid points in each direction are needed to resolve an eddy (since we need adequate resolution of derivatives), we estimate that the total number of grid points for uniform spacing, $N_{uniform}$, is

$$N_{uniform} \approx \left[4\frac{\Lambda}{\eta}\right]^3 = \left[8H\left(\frac{\epsilon}{\nu^3}\right)^{1/4}\right]^3 \tag{8.10}$$

Now, in channel flow, the average dissipation is $\epsilon \approx 2u_\tau^2 U_m/H$ where U_m is the average velocity across the channel, and $U_m/u_\tau \approx 20$. Substituting these estimates into Equation (8.10), we arrive at

$$N_{uniform} \approx (110Re_\tau)^{9/4}, \qquad Re_\tau = \frac{u_\tau H/2}{\nu} \tag{8.11}$$

In practice, it is wasteful to use uniformly spaced grid points since there are regions where ϵ is small and the Kolmogorov length scale is much larger than it is near the surface where ϵ is largest. By using stretched grids to concentrate points where the smallest eddies reside, experience [Moser and Moin (1984), Kim, Moin and Moser (1987)] shows that the factor of 110 in Equation (8.11) can be replaced by about 3. Thus, the actual number of grid points typically used in a DNS of channel flow, N_{DNS}, is

$$N_{DNS} \approx (3Re_\tau)^{9/4} \tag{8.12}$$

Similarly, the timestep in the computation, Δt, should be of the same order as the Kolmogorov time scale, $\tau = (\nu/\epsilon)^{1/2}$. Based on the results of Kim, et al. (1987), the timestep must be

$$\Delta t \approx \frac{.003}{\sqrt{Re_\tau}}\frac{H}{u_\tau} \tag{8.13}$$

To appreciate how prohibitive these constraints are, consider the channel flow experiments done by Laufer (1951) at Reynolds numbers of 12,300, 30,800 and 61,600 and the experiment of Comte-Bellot (1963) at a Reynolds number of 230,000. Table 8.1 lists the number of grid points and timesteps required to perform a DNS, assuming the time required to reach a statistically steady state is $100H/U_m \sim 5H/u_\tau$. Clearly, computer memory limitations make all but the lowest Reynolds number considered by Laufer impractical with computers of the early 1990's. However, it is very impressive indeed that a simulation is feasible for at least one of Laufer's cases.

Table 8.1: Grid point and timestep requirements for channel-flow DNS

Re_H	Re_τ	N_{DNS}	Timesteps
12,300	360	$6.7 \cdot 10^6$	32,000
30,800	800	$4.0 \cdot 10^7$	47,000
61,600	1,450	$1.5 \cdot 10^8$	63,000
230,000	4,650	$2.1 \cdot 10^9$	114,000

The computations of Kim, et al. (1987) provide an example of the computer resources required for DNS of channel flow. To demonstrate grid convergence of their methods, they compute channel flow with $Re_\tau = 180$, corresponding to $Re_H \approx 6,000$ using grids with $2 \cdot 10^6$ and $4 \cdot 10^6$ points. For the finer grid, the CPU time on a Cray X/MP was 40 seconds per timestep, was run for a total time $5H/u_\tau$, and required 250 CPU hours.

Both second-order accurate and fourth-order accurate numerical algorithms have been used in DNS research to advance the solution in time. There are two primary concerns regarding numerical treatment of the spatial directions. The first is achieving accurate representations of derivatives, especially at the smallest scales (or, equivalently, the highest wavenumbers). Spectral methods — Fourier series in the spatial directions — are used to insure accurate computation of derivatives. If derivatives are inaccurate at the smallest scales, excessive energy accumulates in the smallest finite-difference cells, resulting in excessive dissipation. Consequently, the primary issue in demonstrating grid convergence of a DNS is to verify that the energy spectrum, $E(\kappa)$, displays a rapid decay, often referred to as the **rolloff**, near the Kolmogorov length scale, η. While spectral methods are more accurate for computing derivatives at the smallest scales, they are not amenable to arbitrary grid-point spacing. The second issue is to avoid a phenomenon known as **aliasing**. This occurs when nonlinear interactions among the resolved wavenumbers produce waves with wavenumbers greater than κ_{max}, which can be misinterpreted numerically. If special precautions are not taken, this can result in a spurious transfer of energy to small wavenumbers [Ferziger (1976)].

In their grid-convergence study, Kim, et al. (1987) show that their energy spectra display the characteristic rolloff approaching the Kolmogorov length scale. This is true even though their computations actually resolve the flow down to about 2η, rather than to η. This means the actual dissipation results from a combination of the true viscosity and some amount of

numerical viscosity. Although the smallest eddies are not resolved in regions such as the viscous superlayer near the edge of a turbulent/nonturbulent interface, the resolution is fine enough to insure that the rate of dissipation is correctly predicted. Most importantly, the peak dissipation near the surface occurs between 6η and 10η, which is well resolved in the simulation. As in physical turbulence, the smallest eddies in the DNS apparently achieve an equilibrium state in which they dissipate the kinetic energy cascaded from the larger eddies.

As an example of the type of numerical algorithm used in DNS research to advance the solution in time, Kim, et al. (1987), use a procedure very similar to that used in Program EDDYBL (Section 7.3 and Appendix C), viz., Crank-Nicolson differencing for the viscous terms, and the three-point forward difference formulation (Adams-Bashforth) for the convective terms. To improve numerical accuracy for the smallest eddies, the equations are Fourier transformed in the streamwise and spanwise directions. This also permits use of the Fast Fourier Transform (FFT) [Cooley and Tukey (1965)], which is extremely efficient on a computer. Fourier transforms are suitable as the flow can be treated as though it is periodic in these directions. This cannot be done in the direction normal to the surface because of the no-slip boundary condition. Rather, a Chebychev polynomial expansion is used, which yields similar gains in numerical accuracy and computational efficiency. Using Fourier, Chebychev and other eigenfunction expansions, is known as the **spectral method** in its most precise form. A more-efficient approximation exists known as the **pseudo-spectral method**. Spectral and pseudo-spectral methods were pioneered by Orszag, et al. [Patterson and Orszag (1971), Orszag (1972), and Gottlieb and Orszag (1977)].

The primary difficulty with boundary conditions in a DNS is at open boundaries. Because of the elliptic nature of the problem, the flow at such boundaries depends on the unknown flow outside the computational domain. This problem is circumvented by imposing periodic boundary conditions for directions in which the flow is statistically homogeneous (e.g., the streamwise and spanwise directions in channel flow). Flows that grow in the streamwise direction in a nearly self-similar manner (e.g., equilibrium boundary layers) can be reduced to approximate homogeneity by a coordinate transformation [Spalart (1986), Spalart (1988), Spalart (1989)]. Most simulations done to date are homogeneous or periodic in at least two spatial directions. Boundary conditions at a solid boundary pose no special problems where the no-slip velocity boundary condition applies.

Initial conditions are often obtained from results of a previous simulation if available. If no such results are available, a random fluctuating velocity field can be added to a prescribed mean-velocity field. After a few eddy turnover times, the correct statistics ultimately evolve. Interestingly, the

work done to date shows a feature of turbulence that illustrates one of its mysteries. Suppose we have generated a solution from some given set of initial conditions. Suppose further that we make a small perturbation in the initial conditions and repeat the computation. We find that, after a few eddy-turnover times, the second solution, or **realization**, is very different from the first. However, in terms of all statistical measures, the two flows are identical!

This is the classical problem of **predictability** discussed, for example, by Sandham and Kleiser (1992). As a simple example, two strangers in a crowd tend to drift apart. If one steps on another's foot twice, the stepee thinks the stepor does it on purpose, although the cause and effect are completely random. Thus, while somewhat disconcerting to the mathematician, this phenomenon should come as no great surprise to the engineer.

DNS matured rapidly during the 1980's and continues to develop as more and more powerful computers appear. As an example, DNS data are currently available for the following flows, and the list of applications continues to grow.

- Curved channel flow
- Channel flow, with and without heat transfer — values of Re_H as high as 13,750 have been achieved
- Two-dimensional boundary layers in various pressure gradients — values of Re_θ as high as 1,410 have been achieved
- Three-dimensional flows including flow over a swept wing
- Two-dimensional separating and reattaching flows
  - (a) shallow separation bubble on a flat surface
  - (b) flow over a backward-facing step
- Two-dimensional time- and spatially-developing mixing layers
- Three-dimensional Ekman layer
- Two-dimensional buoyant flows
- Two-dimensional homogeneously-strained flows
- Two-dimensional homogeneous flows with constant-density chemical reactions
- Compressible homogeneous flows with bulk compression in one, two or three directions
- Transitional compressible flows

8.3 Large Eddy Simulation

A Large Eddy Simulation, or LES for short, is a computation in which the large eddies are computed and the smallest eddies are modeled. The underlying premise is that the largest eddies are directly affected by the boundary conditions and must be computed. By contrast, the small-scale turbulence is more nearly isotropic and has universal characteristics; it is thus more amenable to modeling.

Because LES involves modeling the smallest eddies, the smallest finite-difference cells can be much larger than the Kolmogorov length, and much larger timesteps can be taken than are possible in a DNS. Hence, for a given computing cost, it is possible to achieve much higher Reynolds numbers with LES than with DNS. Based on a combination of estimates given by Rogallo and Moin (1984) and recent channel-flow LES results of Yang and Ferziger (1993), the number of grid points required for channel flow, N_{LES} should be

$$N_{LES} \approx \left(\frac{0.4}{Re_\tau^{1/4}} \right) N_{DNS} \tag{8.14}$$

Table 8.2 compares grid point requirements based on this estimate. Credible channel-flow results have been obtained with fewer grid points by using the law of the wall to obviate integration through the viscous sublayer. Deardorff (1970), for example has done a LES of Laufer's (1951) $Re_H = 61,600$ channel-flow experiment using just 6,720 mesh points. Schumann (1975) has computed channel flow with $Re_H > 10^4$ using 65,536 points, and the computations even include temperature fluctuations and heat transfer. Grotzbach (1979) has done a LES for buoyancy-driven mixing in a nuclear reactor with $16x16x8 = 2,048$ grid points. In all cases, sensible statistics have been obtained for the largest eddies, although mean-flow properties such as velocity sometimes differ from measurements by as much as 15%. While using the law of the wall as a boundary condition is attractive from a computing-cost point of view, this approach has been abandoned in most recent LES work. No viable scheme has been developed to establish the fluctuating quantities in the log layer, which are needed along with the overall statistics to achieve a suitable boundary condition. As a final comment, although LES is more economical than DNS (typically requiring 5 to 10% of the CPU time needed for DNS), the method still requires large computer resources.

Aside from the issue of the need to resolve the smallest eddies, the comments regarding DNS numerics, boundary and initial conditions in the previous section hold for LES as well. The primary issue in accuracy remains that of computing derivatives at the smallest scales (highest wavenumbers) resolved. The ultimate test of grid convergence is again the requirement

Table 8.2: Grid point requirements for channel-flow DNS and LES

Re_H	Re_τ	N_{DNS}	N_{LES}
12,300	360	$6.7 \cdot 10^6$	$6.1 \cdot 10^5$
30,800	800	$4.0 \cdot 10^7$	$3.0 \cdot 10^6$
61,600	1,450	$1.5 \cdot 10^8$	$1.0 \cdot 10^7$
230,000	4,650	$2.1 \cdot 10^9$	$1.0 \cdot 10^8$

that excessive energy must not accumulate in the smallest scales. The primary requirement is to get the dissipation rate right; details of the dissipating eddies are unimportant in LES. (By contrast, DNS requires accurate simulation of the dissipating eddies.) If spectral or pseudo-spectral methods are used, the same boundary-condition difficulties hold in both DNS and LES.

To understand the primary difference between DNS and LES, we must introduce the concept of **filtering**. To understand this concept, note first that the values of flow properties at discrete points in a numerical simulation represent averaged values. To see this explicitly, consider the central-difference approximation for the first derivative of a continuous variable, $u(x)$, in a grid with points spaced a distance h apart. We can write this as follows.

$$\frac{u(x+h) - u(x-h)}{2h} = \frac{d}{dx}\left[\frac{1}{2h}\int_{x-h}^{x+h} u(\xi)\, d\xi\right] \tag{8.15}$$

This shows that the central-difference approximation can be thought of as an operator that **filters out scales smaller than the mesh size**. Furthermore, the approximation yields the derivative of an averaged value of $u(x)$.

There are many kinds of filters that can be used. The simplest type of filter is the **volume-average box filter** used by Deardorff (1970), one of the earliest LES researchers. The filter is:

$$\overline{u}_i(\mathbf{x}, t) = \frac{1}{\Delta^3}\int_{x-\frac{1}{2}\Delta x}^{x+\frac{1}{2}\Delta x}\int_{y-\frac{1}{2}\Delta y}^{y+\frac{1}{2}\Delta y}\int_{z-\frac{1}{2}\Delta z}^{z+\frac{1}{2}\Delta z} u_i(\boldsymbol{\xi}, t)\, d\xi d\eta d\zeta \tag{8.16}$$

The quantity $\overline{u}_i$ denotes the **resolvable-scale filtered velocity**. The **subgrid scale (SGS)** velocity, u_i', and the **filter width**, Δ, are given by

$$u_i' = u_i - \overline{u}_i \quad \text{and} \quad \Delta = (\Delta x \Delta y \Delta z)^{1/3} \tag{8.17}$$

Leonard (1974) defines a generalized filter as a convolution integral, viz.,

$$\overline{u}_i(\mathbf{x},t) = \iiint G(\mathbf{x}-\boldsymbol{\xi};\Delta)\, u_i(\boldsymbol{\xi},t)\, d^3\boldsymbol{\xi} \tag{8.18}$$

The **filter function**, G, is normalized by requiring that

$$\iiint G(\mathbf{x}-\boldsymbol{\xi};\Delta)\, d^3\boldsymbol{\xi} = 1 \tag{8.19}$$

In terms of the filter function, the volume-average box filter as defined in Equation (8.16) is:

$$G(\mathbf{x}-\boldsymbol{\xi};\Delta) = \begin{cases} 1/\Delta^3, & |x_i - \xi_i| < \Delta x_i/2 \\ 0, & \text{otherwise} \end{cases} \tag{8.20}$$

The Fourier transform of Equation (8.18) is $\overline{U}_i(\kappa,t) = \mathcal{G}(\kappa)\mathcal{U}_i(\kappa,t)$ where $\mathcal{U}_i$ and $\mathcal{G}$ represent the Fourier transforms of u_i and G. Fourier spectral methods implicitly filter with

$$\mathcal{G}(\kappa;\Delta) = 0 \quad \text{for} \quad |\kappa| > \kappa_{max} = 2\pi/\Delta \tag{8.21}$$

As an example, Orszag et al. [see Ferziger (1976)] use

$$G(\mathbf{x}-\boldsymbol{\xi};\Delta) = \frac{1}{\Delta^3}\prod_{i=1}^{3}\frac{\sin(x_i-\xi_i)/\Delta}{(x_i-\xi_i)/\Delta} \tag{8.22}$$

The **Gaussian filter** [Ferziger (1976)] is popular in LES research, and is defined by

$$G(\mathbf{x}\text{-}\boldsymbol{\xi};\Delta) = \left(\frac{6}{\pi\Delta^2}\right)^{3/2}\exp\left(-6\,\frac{|\mathbf{x}-\boldsymbol{\xi}|^2}{\Delta^2}\right) \tag{8.23}$$

Many other filters have been proposed and used, some of which are neither isotropic nor homogeneous. In all cases however, the filter introduces a scale Δ that represents the smallest turbulence scale allowed by the filter.

The filter provides a formal definition of the averaging process and separates the **resolvable scales** from the **subgrid scales**. We use filtering to derive the **resolvable-scale equations**. For incompressible flow, the continuity and Navier-Stokes equations assume the following form.

$$\frac{\partial \overline{u}_i}{\partial x_i} = 0 \tag{8.24}$$

$$\frac{\partial \overline{u}_i}{\partial t} + \frac{\partial}{\partial x_j}\left(\overline{u_i u_j}\right) = -\frac{1}{\rho}\frac{\partial \overline{p}}{\partial x_i} + \nu\frac{\partial^2 \overline{u}_i}{\partial x_k \partial x_k} \tag{8.25}$$

Now, the convective flux is given by

$$\overline{u_i u_j} = \overline{u}_i \overline{u}_j + L_{ij} + C_{ij} + R_{ij} \tag{8.26}$$

where

$$\left.\begin{aligned} L_{ij} &= \overline{\overline{u}_i \overline{u}_j} - \overline{u}_i \overline{u}_j \\ C_{ij} &= \overline{\overline{u}_i u_j'} + \overline{\overline{u}_j u_i'} \\ R_{ij} &= \overline{u_i' u_j'} \end{aligned}\right\} \tag{8.27}$$

Note that filtering differs from standard averaging in one important respect:

$$\overline{\overline{u}}_i \neq \overline{u}_i \tag{8.28}$$

i.e., a second averaging yields a different result from the first averaging. The tensors L_{ij}, C_{ij} and R_{ij} are known as the **Leonard stress**, **cross-term stress** and the **SGS Reynolds stress**, respectively.

Leonard (1974) shows that the Leonard stress term removes significant energy from the resolvable scales. It can be computed directly and needn't be modeled. This is sometimes inconvenient however, depending on the numerical method used. Leonard also demonstrates that since $\overline{u}_i$ is a smooth function, L_{ij} can be computed in terms of its Taylor series expansion, the first term of which is

$$L_{ij} \approx \frac{\gamma_\ell}{2} \nabla^2 \left(\overline{u}_i \overline{u}_j \right), \qquad \gamma_\ell = \iiint |\boldsymbol{\xi}|^2 G(\boldsymbol{\xi})\, d^3\boldsymbol{\xi} \tag{8.29}$$

Clark, et al. (1979) verify that this representation is very accurate at low Reynolds number by comparing with DNS results. However, as shown by Shaanan, Ferziger and Reynolds (1975), the Leonard stresses are of the same order as the truncation error when a finite-difference scheme of second-order accuracy is used, and are thus implicitly represented.

The cross-term stress tensor, C_{ij}, also drains significant energy from the resolvable scales. An expansion similar to Equation (8.29) can be made for C_{ij}. However, most current efforts model the sum of C_{ij} and R_{ij}. Clearly, the accuracy of a LES depends critically upon the model used for these terms.

We can now rearrange Equation (8.25) into a more conventional form, i.e.,

$$\frac{\partial \overline{u}_i}{\partial t} + \frac{\partial}{\partial x_j} \left(\overline{u}_i \overline{u}_j \right) = -\frac{1}{\rho} \frac{\partial P}{\partial x_i} + \frac{\partial}{\partial x_j} \left[\nu \frac{\partial \overline{u}_i}{\partial x_j} + \frac{\tau_{ij}}{\rho} \right] \tag{8.30}$$

where

$$\left.\begin{aligned} \frac{\tau_{ij}}{\rho} &= -\left(Q_{ij} - \tfrac{1}{3} Q_{kk} \delta_{ij} \right) \\ P &= \overline{p} + \tfrac{1}{3} \rho Q_{kk} \delta_{ij} \\ Q_{ij} &= R_{ij} + C_{ij} \end{aligned}\right\} \tag{8.31}$$

At this point, **the fundamental problem of Large Eddy Simulation** is evident. Specifically, we must establish a satisfactory model for the SGS stresses as represented by the tensor Q_{ij}. To emphasize the importance of achieving an accurate SGS stress model, consider the following. In simulating the decay of homogeneous isotropic turbulence with $16^3 = 4,096$ and $32^3 = 32,768$ grid points, Ferziger (1976) reports that the SGS turbulence energy is 29% and 20%, respectively, of the total. Thus, the subgrid scales constitute a significant portion of the turbulence spectrum. The various attempts at developing a satisfactory SGS stress model during the past four decades resemble the research efforts on engineering models discussed in Chapters 3 - 6. That is, models have been postulated that range from a simple gradient-diffusion model [Smagorinsky (1963)], to a one-equation model [Lilly (1966)], to the analog of a second-order closure model [Deardorff (1973)]. Nonlinear stress-strain rate relationships have even been postulated [Bardina, Ferziger and Reynolds (1983)]. Only the analog of the two-equation model appears to have been overlooked, most likely because the filter width serves as a readily available length scale.

Smagorinsky (1963) was the first to postulate a model for the SGS stresses. The model assumes the SGS stresses follow a gradient-diffusion process, similar to molecular motion. Consequently, τ_{ij} is given by

$$\tau_{ij} = 2\mu_T S_{ij}, \qquad S_{ij} = \frac{1}{2}\left(\frac{\partial \overline{u}_i}{\partial x_j} + \frac{\partial \overline{u}_j}{\partial x_i}\right) \tag{8.32}$$

where the **Smagorinsky eddy viscosity** is

$$\mu_T = \rho(C_S\Delta)^2\sqrt{S_{ij}S_{ij}} \tag{8.33}$$

and C_S is the Smagorinsky coefficient.

For all of the reasons discussed in Chapter 3, the approximation that the smallest eddies behave like molecules is just not true. They are constantly interacting in a much more complicated manner than the infrequent collisions of molecules. Nevertheless, just as the mixing-length model can be readily calibrated for a given class of flows, so can the Smagorinsky coefficient, C_S. As with the mixing-length model, the value of C_S is not universal. Its value varies from flow to flow, and various applications have been done with [Rogallo and Moin (1984)]:

$$0.10 < C_S < 0.24 \tag{8.34}$$

There are two key reasons why the Smagorinsky model has enjoyed some degree of success. First, the model yields sufficient diffusion and dissipation to stabilize the numerical computations. Second, low-order statistics of the larger eddies are usually insensitive to the SGS motions.

In an attempt to incorporate some representation of the dynamics of the subgrid scales and to account for **backscatter** (reverse cascading of energy from smaller to larger eddies), Lilly (1966) postulates that

$$\mu_T = \rho C_L \Delta q \tag{8.35}$$

where q^2 is the SGS kinetic energy, and C_L is a closure coefficient. An equation for q^2 can be derived from a moment of the Navier-Stokes equation, which involves several terms that must be modeled. This model is very similar to Prandtl's one-equation model (Section 4.2), both in spirit and in results obtained. As pointed out by Schumann (1975) who used the model in his LES research, it is difficult to conclude that any significant improvement over the Smagorinsky model can be obtained with such a model.

The most complicated SGS model has been created by Deardorff (1973) for application to the atmospheric boundary layer. The model consists of 10 partial differential equations and bears a strong resemblance to a second-order closure model. While the model leads to improved predictions, its complexity has discouraged many researchers. This is similar to the situation with the second-order closure models discussed in Chapter 6.

Germano, et al. (1990) [see also Ghosal et al. (1992)], have devised an interesting new concept that they describe as a **Dynamic SGS Model**. Their formulation begins with the Smagorinsky eddy-viscosity approximation. However, rather than fixing the value of C_S a priori, they permit it to be computed as the LES proceeds. This is accomplished by using two filters. Yang and Ferziger (1993) present compelling evidence that this approach has great potential in their recent computations of flow over a rectangular obstacle in a channel.

Erlebacher, et al. (1987) have pushed the frontiers of LES research into compressible flows. They have formulated a compressible flow SGS model and exercised it in computation of compressible isotropic turbulence. Results obtained are in excellent agreement with DNS results.

In conclusion, LES holds promise as a future design tool, especially as computers continue to increase in speed and memory. Intense efforts are currently focused on devising a satisfactory SGS stress model, which is the primary deficiency of the method at this time. Even if LES is too expensive for modern design efforts, results of LES research can certainly be used to help improve engineering models of turbulence. The future of LES research appears very bright.

8.4 Chaos

Our final topic is chaos, a mathematical theory that has attracted considerable attention in recent years. At the present time, no quantitative predictions for properties such as the reattachment length behind a backward-facing step or even the skin friction on a flat plate have been made. Hence, its relevance to turbulence modeling thus far has not been as a competing predictive tool. Rather, the theory's value is in developing qualitative understanding of turbulent flow phenomena.

Chaos abounds with colorful terminology including **fractals**, **folded towel diffeomorphisms**, **smooth noodle maps**, **homeomorphisms**, **Hopf bifurcation** and the all important **strange attractor**. Chaos theory stretches our imagination to think of noninteger dimensional space, and abounds with marvelous geometrical patterns with which the name Mandelbrot is intimately connected.

In the context of turbulence, the primary focus in chaos is upon **nonlinear dynamical systems**, i.e., a coupled system of nonlinear ordinary differential equations. Mathematicians have discovered that certain dynamical systems with a very small number of equations (degrees of freedom) possess extremely complicated (chaotic) solutions. Very simple models have been created that simulate observed physical behavior for nontrivial problems. For example, consider an initially motionless fluid between two horizontal heat-conducting plates in a gravitational field. Now suppose the lower plate is heated slightly. For small temperature difference, viscous forces are sufficient to suppress any mass motion. As the temperature is increased, a threshold is reached where fluid motion begins. A series of convective rolls forms that becomes more and more complicated as the temperature increases, and the flow ultimately becomes turbulent. This is known as **Rayleigh-Bénard instability** or **Rayleigh-Bénard convection**.

One of the famous successes of chaos theory is in describing this phenomenon with the following three coupled **ordinary** differential equations.

$$\left.\begin{aligned} \frac{dX}{dt} &= (Y - X)/Pr_L \\ \frac{dY}{dt} &= -XZ + rX - Y \\ \frac{dZ}{dt} &= XY - bZ \end{aligned}\right\} \tag{8.36}$$

The quantity Pr_L is the Prandtl number, b and r are constants, and X, Y and Z are related to the streamfunction and temperature. The precise details of the model are given by Bergé, Pomeau and Vidal (1984), and are not important for the present discussion. What is important is the

following. This innocent looking set of equations yields a qualitative analog to the Rayleigh-Bénard convection problem, including the geometry of the convection rolls and a solution that resembles turbulent flow.

The central feature of these equations is that they describe what is known as a strange attractor. This particular attractor was the first to be discovered and is more specifically referred to as the **Lorenz attractor**. For the general case, in some suitably defined **phase space** in which each point characterizes the velocity field within a three-dimensional volume (X, Y and Z for the Lorenz attractor), the dynamical system sweeps out a curve that we call the attractor. The concept of a phase space is an extension of classical phase-plane analysis of ordinary differential equations [c.f. Bender and Orszag (1978)]. In phase-plane analysis, for example, linear equations have critical points such as the focus, the node and the saddle point. For a dynamical system, if the flow is steady, the curve is a single point, as the velocity is independent of time. If the flow is periodic the curve is closed and we have the familiar limit cycle. The interesting case in chaos is the unsteady, aperiodic case in which the curve asymptotically approaches the strange attractor. If the dynamical system is dissipative, as the Lorenz equations are, the solution trajectories always converge toward an attractor. Additionally, a slight change in the initial conditions for X, Y and Z causes large changes in the solution.

Chaos theory puts great emphasis on the strange attractor, and one of the primary goals of chaos research is to find a set of equations that correspond to the **turbulence attractor**. A dynamical regime is chaotic if two key conditions are satisfied:

1. Its power spectrum contains a continuous part, i.e., a broad band, regardless of the possible presence of peaks.

2. The autocorrelation function goes to zero in finite time.

Of course, both of these conditions are characteristic of turbulence. The latter condition means there is ultimately a loss of memory of the signal with respect to itself. This feature of chaos accounts for the strange attractor's **sensitive dependence on initial conditions**. That is, on a strange attractor, two neighboring trajectories always diverge, regardless of their initial proximity, so that the trajectory actually followed by the system is very sensitive to initial conditions. In chaos, this is known as the **butterfly effect** — the notion that a butterfly flapping its wings in Beijing today can change storm systems in New York next month. It is also precisely what has been observed about the sensitivity of DNS and LES to initial conditions.

While all of these observations indicate there may be promise in using chaos to tackle the turbulence problem, there are some sobering realities

that must be faced. The broad spectrum of wavelengths in the turbulence spectrum, ranging from the Kolmogorov length scale to the dimension of the flow, is far greater than that of the dynamical systems that have been studied. Hence, as deduced by Keefe (1990) from analysis of DNS data, the dimension of the turbulence attractor (in essence, the number of equations needed to describe the attractor) must be several hundreds for Reynolds numbers barely large enough for turbulence to exist. As noted by Bradshaw (1992), "the most ambitious efforts require an amount of computing time which is not much less than that of a large-eddy simulation."

The layman oriented book by Gleick (1988) provides an excellent introduction to this fascinating theory in general. As a more focused reference, Deissler (1989) presents a review of chaos studies in fluid mechanics.